

1 **Extreme sensitivity of the northeastern Gulf of Lion (western Mediterranean)**  
2 **to subsurface heatwaves: Physical processes and insights into effects on**  
3 **gorgonian populations in the summer of 2022**

4 Claude Estournel<sup>1</sup>, Tristan Estaque<sup>2</sup>, Caroline Ulses<sup>1</sup>, Quentin-Boris Barral<sup>1</sup>, Patrick Marsaleix<sup>1</sup>

5 <sup>1</sup>Université de Toulouse, LEGOS (CNES/CNRS/IRD/UT3), Toulouse, France

6 <sup>2</sup>Septentrion Environnement, Marseille, France

7 *Correspondence to:* Claude Estournel (claude.estournel@cnrs.fr)

8 **Abstract.** In the summer of 2022, atmospheric conditions characterized by persistent anticyclonic anomaly caused an  
9 extreme marine heatwave in the western Mediterranean Sea. Time series of temperature profiles at various points along the  
10 northeastern coast of the Gulf of Lion (NW Mediterranean Sea) showed exceptional temperatures down to depths of 30 m  
11 which led to massive mortality of benthic species. A hydrodynamic numerical simulation was used to analyze the physical  
12 processes responsible for this subsurface heatwave in a region where the climatology in summer is characterized by  
13 northerly winds inducing upwelling alternating with low winds. Firstly, the recurrence of heatwaves limited to the surface is  
14 demonstrated, triggered when upwelling stopped and warm water from the Northern Current intruded on the shelf. More  
15 importantly, in August and early September 2022, two episodes of southerly and easterly winds of 8 to 10 m·s<sup>-1</sup> occurred.  
16 The oceanic response to these winds was an alongshore cyclonic current advecting warm water onto the shelf and a  
17 downwelling of this warm water to depths of the order of 30 to 40 m. A large part of the Gulf of Lion coast was warmed by  
18 these events. However, the northeastern part of the shelf, on either side of the city of Marseille, was by far the area most  
19 affected in depth, due to the combination of the proximity of the warm surface waters of the Ligurian coast advected by  
20 wind-induced currents and the local acceleration of the wind by the continental topography, which intensifies the  
21 downwelling of these surface waters. These events are rare in summer, but their impact on the rich benthic ecosystems that  
22 characterize the region is dramatic, and will only increase with the warming trend in surface waters, already close to 1 °C for  
23 the last decade.

24 **1 Introduction**

25 With global warming, the number, intensity and duration of marine heatwaves (MHW) are on the rise, and MHW events  
26 occur throughout the year (Fox-Kemper et al., 2021). Impacts on marine organisms are likely to be most marked in coastal  
27 areas. Benthic communities, being sedentary or having only limited mobility, are indeed particularly vulnerable to extreme

temperatures (Lejeusne et al., 2010; Hughes et al., 2017; Garrabou et al., 2022) rather than to the exceedance of climatological values likely to occur throughout the year. This is the case for coral, for example, with a bleaching threshold defined for the Hawaiian Islands when surface temperature exceeds the maximum monthly mean by 1 degree (Glynn and D'Croz, 1990). When biological impacts are considered, it is therefore summer heatwaves that should be particularly monitored.

While surface MHW have been documented over several decades from satellite SSTs (Sea Surface Temperatures), in-situ data documenting temperatures in the first few tens of meters below the surface are infrequent, and their spatial representativeness varies greatly from site to site, particularly in coastal areas which are subject to unique dynamical processes due to the shallow depths and proximity to land (Schaeffer et al., 2023). On the one hand, irregularities in the coastline and submarine topography condition horizontal alongshore and cross-shore exchanges; on the other hand, spatial variations in the wind (possibly related to continental relief) can generate localized coastal upwelling and downwelling depending on the orientation of the coastline relative to the wind direction. In contrast to upwelling, which counteracts the occurrence and intensity of heatwaves in the first few tens of meters of the water column (defined here as the sub-surface) and is identifiable on the SST, downwelling favors the penetration of warm surface water at depth, possibly beneath the stratified surface layer, and is generally not identifiable from the SST, especially as surface water can be cooled by air-sea heat fluxes (Schaeffer et al., 2023). Tracking coastal subsurface heatwaves is therefore impossible using surface information alone. As underlined by Schaeffer et al. (2023), the best proxy of sub-surface temperature extremes appears to be wind anomalies since sub-surface MHW events and years characterized by many sub-surface MHW days are predominantly associated with wind-driven downwelling. Numerical models are the only way to document them at high spatial (horizontal and vertical) and temporal resolution. However, their accuracy is a prerequisite when it comes to exceeding a tolerance threshold.

Since 1982, the Mediterranean SST has been warming at a mean rate of  $\sim 0.35$  °C/decade (Pastor et al., 2020), compared with the global mean increase of 0.15 °C/decade (Fox-Kemper et al., 2021). For the 2010-2019 decade, Garrabou et al. (2022) showed an increase in warming for an average of seven coastal sites in the north-western Mediterranean Sea, with values for the decade of 0.9 °C at 5 m and 0.6 °C at 35-40 m. Superimposed on this long-term warming, several authors have noted increased frequency, intensity and duration of MHW over the last four decades (Simon et al., 2022; Juza et al., 2022; Pastor et al., 2023) and an acceleration in recent years. Recently an exceptionally long-lasting and intense MHW, started in May 2022 (Martinez et al., 2023) and persisted until spring 2023 (Marullo et al., 2023). According to the latter authors, the intensity of this MHW was comparable to that of the 2003 event, which is the most intense case ever occurred in the last decades. The 2022 MHW was attributed to an atmospheric heatwave in Western Europe due to a persistent anticyclonic anomaly (Guinaldo et al., 2023) exacerbated by climate change (Faranda et al., 2023). Never-before-recorded

61 temperatures were observed at the surface of the western Mediterranean Sea during this summer (Guinaldo et al., 2023). In  
62 the Marseille area, east of the Gulf of Lion, temperatures exceeded 26 °C at 20 m for 4 days in August and 25 °C down to 30  
63 m for 3 days in early September (see more details in Grenier et al., 2022; Estaque et al., 2023). Following these last authors,  
64 depths from 25-30 m were exposed for the very first time to temperatures above 25 °C, considered as a potentially lethal  
65 acute heat stress threshold for benthic species (Crisci et al., 2011).

66

67 During the heatwaves of 1999 and 2003, large scale (>1000 km coastline) mass mortality events have affected numerous  
68 species of benthic invertebrates in the north-western Mediterranean Sea (Bensoussan et al., 2010 and references herein)  
69 indicating that they are living near their upper thermal thresholds. In the Parc National des Calanques south-east of  
70 Marseille, high temperatures in the summer of 2022 had an unprecedented impact on the mortality of numerous species,  
71 especially for the red gorgonian, *Paramuricea clavata*, and the red coral, *Corallium rubrum*, affecting depths down to 30 m  
72 (Estaque et al., 2023). Other emblematic species, such as sponges, have totally disappeared around Marseille at depths of  
73 down to 25 m, with only a few individuals surviving between 25 and 30 m (Grenier et al., 2022). The first sponge mortalities  
74 were recorded when temperatures exceeded 26 °C.

75

76 The aim of this article is to understand the interweaving of physical mechanisms from the large to the local scale at the origin  
77 of the summer 2022 subsurface heatwave, extreme in its intensity and impacts in the region of Marseille. To achieve this, we  
78 use numerical modeling checked against a dense network for top 40 m temperature measurement, called TMED-Net, which  
79 documents surface and subsurface heatwaves.

80

## 81 **2 Main characteristics of the study site**

82 The Gulf of Lion (Fig. 1) comprises a broad, crescent-shaped continental shelf enclosed between two straight coasts, the  
83 Ligurian coast to the northeast and the Catalan coast to the southwest, bordered by a narrow shelf and a steep continental  
84 slope, along which the Northern Current transports from northeast to southwest warm and low salinity waters from the south  
85 of the western Mediterranean basin and originally from the Atlantic. Under certain meteorological conditions, the Northern  
86 Current splits into two branches, the coastal branch entering the continental shelf along the coast (Barrier et al., 2016; Ross  
87 et al., 2016). These intrusions occur particularly under stratified conditions.

88

89

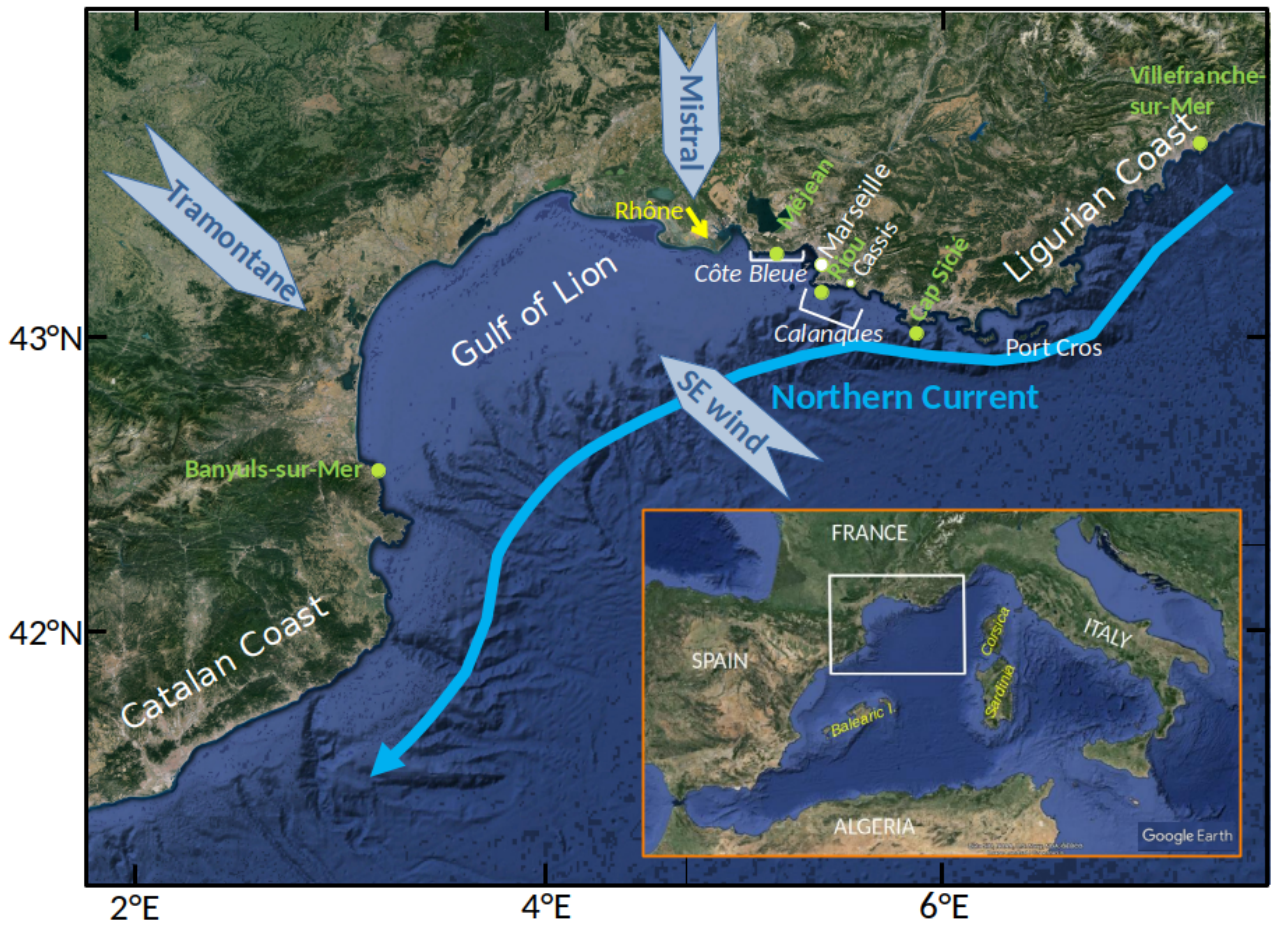


**Figure 1: Location and topography of the study area (background map from Google Earth). The prevailing Mistral and Tramontane winds, the southeast wind, the Northern Current, regional branch of the general circulation are indicated as well as the different places named in the text. The green solid circles indicate the TMED-Net observation points, Méjean, Banyuls-sur-Mer and Villefranche-sur-Mer on which comparisons with the model are focused, and Riou and Cap Sicié. The insert is a more general map of the western Mediterranean Sea, in which the area is indicated by a white rectangle.**

The north-western Mediterranean Sea is a mosaic of contrasting hydrological situations due to bathymetric constraints and complex wind regimes. In the Gulf of Lion, the prevailing winds blow from land (north to northwest, referred to in the following as the northerly winds for simplicity's sake) and are channeled by orography, the Rhone valley to the north, where the Mistral blows, and the passage between the Pyrenees and the Massif Central to the west, where the Tramontane blows. As a result, winds are much stronger in the Gulf of Lion than along the Catalan and Ligurian coasts. These northerly winds produce discontinuous coastal upwelling to the north of the zone, from around 3.5°E to 5.8°E (Millot, 1990), leading to surface cooling in summer that can exceed 10 °C in 1 to 2 days (Odic et al., 2022). Using criteria not detailed here, based on

the temperature anomaly with respect to climatology and the cooling between two successive days, the frequency of these events near Marseille between 2012 and 2022 averages 6.3 per summer (Barral pers. comm.). For Tramontane, the west coast is on the contrary favorable to downwelling (Bensoussan et al., 2010; Odic et al., 2022), producing less variable surface temperatures but nevertheless presenting lower maximum values than to the east (Pairaud et al., 2014) due to an increase in wind intensity and frequency from east to west (Obermann-Hellhund et al., 2018) and a reduced influence of the warm Northern Current.

109

After these northerly winds, the second type of winds blows from southwest to southeast, but locally these winds are strongly influenced by the relief of the islands and the mainland, which can strongly modify their intensity and direction. They generally enter the Gulf of Lion from a direction that varies from east after following the Ligurian coast, to southeast as they bypass Corsica and Sardinia, and to south. In what follows, we will refer to these winds as southeasterly winds in accordance with several authors (e.g. Millot, 1990; Odic et al., 2022). Rare in July-August, their frequency and intensity then increase sharply to peak in October-November (Odic et al., 2022), when it is frequently accompanied by precipitation on the mainland, which can lead to flash flooding of rivers, possibly accompanied by significant material and human damage (Ducrocq et al., 2014; Drobinski et al., 2014). These winds, which can reach  $25 \text{ m}\cdot\text{s}^{-1}$  in winter, induce cyclonic circulation around the Gulf of Lion, with currents of several tens of  $\text{cm}\cdot\text{s}^{-1}$ , accompanied by intensified downwelling to its southwestern tip due to the acceleration of currents linked to the narrowing of the continental shelf (Ulses et al., 2008; Mikolajczak et al., 2020).

121

The region around Marseille includes to the east the “Parc National des Calanques”, characterized by remarkable marine habitats (e.g. *Posidonia* meadows, coralligenous reefs, semi-dark caves, submarine canyons), 14 of which are considered rare and fragile (<https://www.calanques-parcnational.fr/en/marine-habitats>) and which presents a high risk of mass mortality associated to thermal stress for the red gorgonian (Pairaud et al., 2014) as well as for other cnidarians, numerous sponge species, bryozoans and tunicates. To the west of Marseille, the “Parc Marin de la Côte Bleue” is another marine protected area, also hosting a great marine biodiversity similar to that found in the “Parc National des Calanques”, but at relatively shallower depths. In this last area, the presence of remarkable mesophotic ‘giant’ *Paramuricea clavata* forests is particularly noticeable (Sartoretto et al., 2023).

### 130 3 Material and Methods

We use a numerical simulation of the entire Mediterranean basin similar to that described in Estournel et al. (2021). The simulation is based on the 3D primitive equations SYMPHONIE model described in Marsaleix et al. (2008, 2006) and Damien et al. (2017), with turbulence closure and convection parameterization detailed in Estournel et al. (2016). The VQS (vanishing quasi-sigma) vertical coordinate (Estournel et al., 2021) is used with 60 levels. The horizontal resolution in the

135 area of interest is around 1900 m, which may seem coarse for an application very close to the coast, but has proved sufficient  
136 to represent rapid temperature variations, as will be shown in section 4.1 devoted to simulation evaluation (Fig. 2 and 3).  
137 The model was initialized and forced in the Gulf of Cadiz (Atlantic Ocean) from daily operational oceanic analysis produced  
138 by MERCATOR OCEAN International. At the surface it was forced from the 12 hourly forecasts that follow the 00.00 and  
139 12.00 analyses of the ECMWF operational meteorological model. COARE bulk formulas were used to compute the turbulent  
140 air/sea fluxes. The simulation was initialized in May 2011. Comparisons with monthly satellite SST taken at two seasons, 6  
141 and 7 years after model initialization, show a very good representation of large-scale features present in the whole basin but  
142 also of various smaller structures (Estournel et al., 2021).

143

144 At the coastal scale, the simulation is compared with TMED-Net (<https://t-mednet.org/>) observations taken at an hourly  
145 frequency every 5 m between 5 m and 40 m with autonomous sensors fixed to the seabed rocky substrate. This region  
146 includes various TMED-Net observation points stretching from the Côte Bleue to Cap Sicié. For our study, we focused on  
147 the Méjean site located 10 km west of Marseille (Fig. 1), where subsurface warming was generally strongest. We also took a  
148 broader view of the north-western Mediterranean Sea, in order to visualize the specificity of the Marseille region. To do this,  
149 we compared temperature trends at Méjean with those recorded at TMED-Net points in Banyuls-sur-Mer and Villefranche-  
150 sur-Mer, located around 200 km to the south-west and north-east of Marseille (locations on Fig. 1). As mentioned in section  
151 2, Banyuls-sur-Mer on the west coast of the Gulf of Lion is subject to frequent downwellings, and Villefranche-sur-Mer on  
152 the Ligurian coast is strongly impacted by the Northern Current.

153

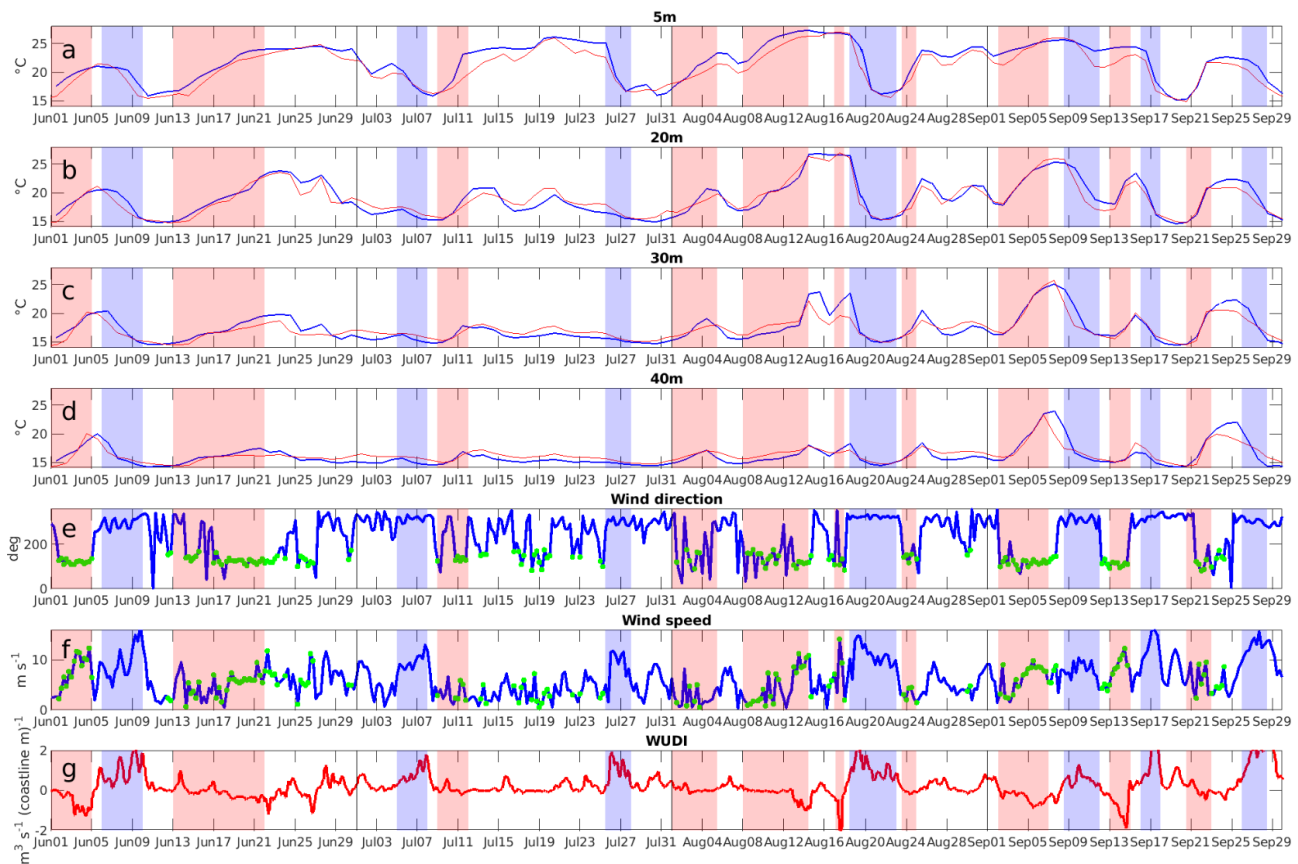
154 To link the intensity of the 2022 MHW with the extreme impacts observed on benthic communities to depths down to 30 m,  
155 we used a compiled dataset acquired by scientists and marine protected area managers in 2022, after the MHW. This dataset  
156 is the largest available for monitoring a mass mortality event for benthic organisms in the Mediterranean Sea. The in-situ  
157 data was acquired using the methods detailed by Estaque et al. (2023), who analyzed some of the data in detail for the “Parc  
158 National des Calanques” area. Here, the dataset consists of in-situ data on the health of 18,465 colonies of red gorgonian (*P.*  
159 *clavata*), white gorgonian (*Eunicella singularis*) and yellow gorgonian (*Eunicella cavolini*), from 298 populations dwelling  
160 between the surface and 40 m depth. The data used allow us to compare the impact between the “Parc National des  
161 Calanques” (PnCal), the “Parc Marin de la Côte Bleue” (PMCB), the “Cap Sicié” (CS), and the “Parc National de Port-Cros”  
162 (PNPC), in relation to the differences in intensity of the 2022 MHW event.

## 163 **4 Results**

### 164 **4.1 Assessment of the simulation and hydrological characteristics during summer 2022**

165 Figure A1 (Appendix A) shows the temporal evolution of measured and simulated temperature at Méjean between 5 and 40  
166 m and between 2012 and 2022. The simulation shows a cold bias of around 0.5°C at all levels, with uneven performance

167 from year to year, particularly at 20 m depth, suggesting an uncertainty in the representation of the thermal gradient of the  
 168 highly stratified layer beneath the surface mixed layer. The correlations between the observed and simulated series are above  
 169 0.95. Rapid temperature variations in summer, reflecting the succession of upwelling and stratification events, are visible at  
 170 all levels and are well synchronized, indirectly indicating a correct representation of wind in the simulation. The maximum  
 171 of the series at 5 m is 27.8 °C in hourly values, reached in August 2022 (28.5 °C at Riou 20 km further south, sea location on  
 172 Fig. 1). The duration of exceedance of the 25 °C value in 2022 is also the longest of the decade. The simulation agrees with  
 173 observations on these two extremes of temperature and duration.  
 174  
 175 Figures 2a to 2d zoom in on Fig. A1 from June to the end of September 2022. Correlations between observed and simulated  
 176 series range from 0.88 at 40 m to 0.96 at 5 m. The model bias is greatest at 5 m (-1 °C) and varies between -0.18 and 0.15  
 177 °C at deeper levels. Warming episodes, highlighted in red, correspond to periods of continuous warming of at least 5 °C  
 178 either at the surface or at 20 m. Northerly winds inducing cooling episodes are highlighted in blue when they reach 10 m·s<sup>-1</sup>.  
 179



180

181 **Figure 2: Observed (blue) and simulated (red) daily averaged temperature time series at the Méjean point of the TMED-Net**  
 182 **network during the summer of 2022 (June to September), from 5 m to 40 m, as indicated above the figures a-d. Wind direction and**

13  
 14

183 intensity (6-hour moving average) near Marseille, from the ECMWF model (ocean model forcing) : e and f. The southeasterly  
184 winds are indicated in green. Wind-induced Upwelling and Downwelling Index (6-hour moving average) calculated at Méjean (g).  
185 Warm events are highlighted by red stripes and northerly winds associated with cooling by blue stripes.

186 Events above 25 °C at 5 m followed one another from July 19 to September 9, with contrasting signatures further down. The  
187 event that peaked at the surface on July 19 resulted in an increase of around 3 °C at 20 m, but was much less pronounced at  
188 greater depths. In contrast, the mid-August event was almost as warm at 20 m as at 5 m, with a signature at 30 m on August  
189 14, shortly after the surface maximum, around +8 °C compared to the beginning of the event. The temperature during the  
190 early September event was almost uniform down to 30 m ( $T > 25$  °C) and reached 24 °C at 40 m.

191

192 Figure 3 compares the local characteristics of the subsurface heatwave observed by the TMED-Net network and simulated  
193 along the anticlockwise pathway of the Northern Current at Villefranche-sur-Mer, Méjean, Banyuls-sur-Mer. In contrast to  
194 Méjean, Villefranche-sur-Mer's summer temperatures in 2022 did not vary greatly. The warm period extends over more than  
195 two months and generally involves a well-stratified surface layer. In Banyuls-sur-Mer, surface water temperatures are also  
196 more continuous than in Méjean, but significantly lower than in Villefranche. On the other hand, the heat is distributed over  
197 a much thicker layer, evoking the recurrent presence of downwellings. The simulation reproduces the thermal regime at the  
198 various sites with shortcomings such as the underestimation of the surface layer temperature at Villefranche-sur-Mer.

#### 199 4.2 Meteorological characteristics during summer 2022

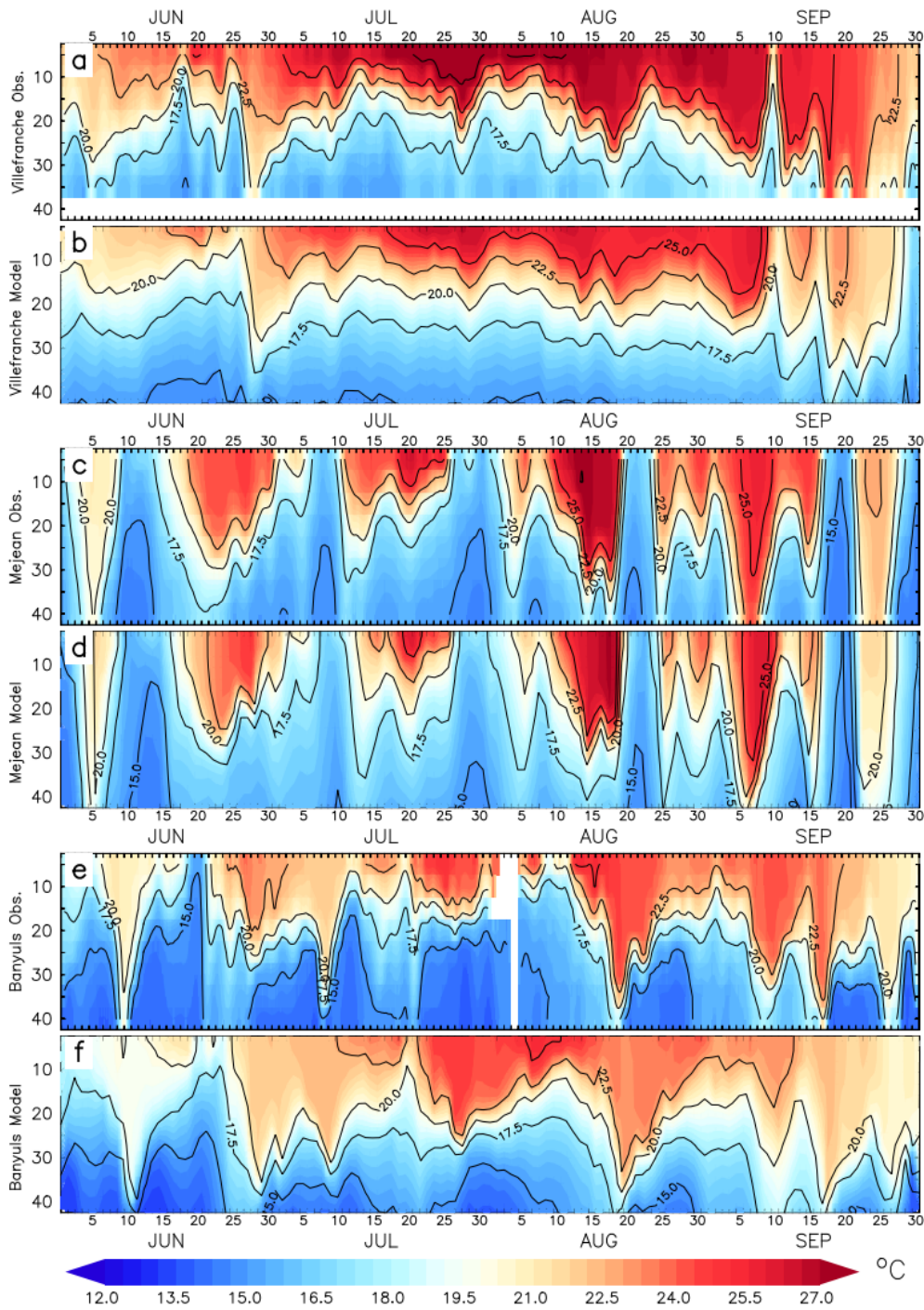
200 Figures 2 e,f show the wind direction and intensity of ECMWF model near Marseille. For greater visual clarity, hourly winds  
201 are averaged over 6 hours. Figure 2g illustrates the wind-induced upwelling and downwelling index (WUDI), as outlined by  
202 Odic et al. (2022), calculated with the ECMWF at the Méjean probe location. This index quantifies the horizontal Ekman  
203 transport within the model, exhibiting a positive or negative value, indicative of upwelling or downwelling, respectively. In  
204 line with climatology, the strongest winds blow from the mainland. Whenever the north, northwest wind exceeds  $10 \text{ m}\cdot\text{s}^{-1}$ , a  
205 surface temperature drop of at least 5 °C is observed and simulated over the following days. This is the case for events  
206 starting on June 6, July 5 and 26, August 18, September 9, 16 and 26. These upwellings are also visible below the surface  
207 (especially if warming has taken place beforehand, as in the cases of June 6 and September 9). In this respect, it's worth  
208 noting that temperatures drop at depth around 24 hours before at the surface (see for example the June 6 event). In all of the  
209 aforementioned instances, the WUDI is greater than  $+0.5 \text{ m}^3\cdot\text{s}^{-1}\cdot(\text{coastline m})^{-1}$ , which is consistent with the previous  
210 identifications of upwelling.

211

212 During summer 2022, warm events are characterized by lower wind intensities than northerly wind events. They are  
213 classified here as either weak winds (typically below  $5 \text{ m}\cdot\text{s}^{-1}$ ), or moderate southeasterly winds (typically above  $5 \text{ m}\cdot\text{s}^{-1}$  and  
214 rarely above  $10 \text{ m}\cdot\text{s}^{-1}$ ). All cases of weak or moderate southeasterly winds are indicated in green in Fig. 2 e,f and are all  
215 located in warm periods. Specifically, the periods in question are June 1-5, 13-22, July 9-12, August 1-4, 8-14, 23-25, and



216 September 2-7, 13-15. For moderate wind speeds, the negative WUDI index below  $-0.5 \text{ m}^3 \cdot \text{s}^{-1} \cdot (\text{coastline m})^{-1}$  suggests a  
 217 potential contribution of downwellings to warming episodes.



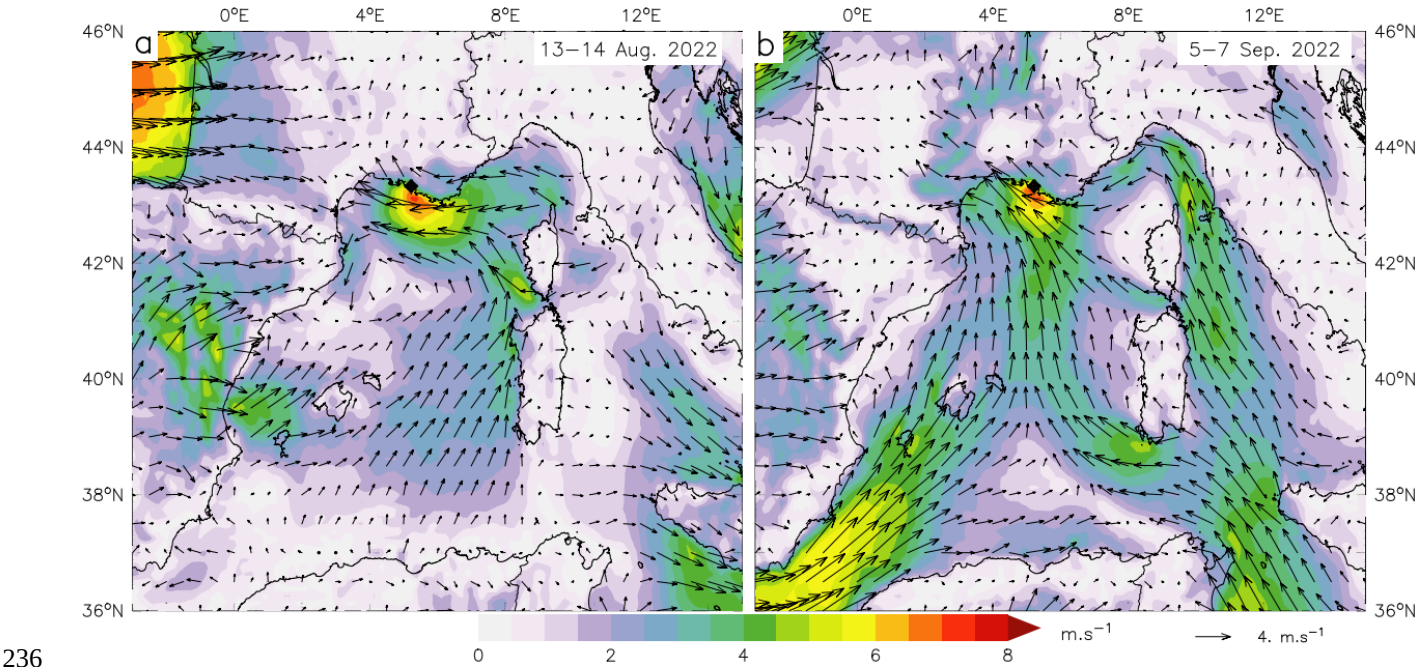
218

17  
18

219 **Figure 3: Hovmöller diagrams of the temperature ( $^{\circ}\text{C}$ ) profiles (m) given by the TMED-Net probes (a, c, e) and the model (b, d, f)**  
 220 **at the locations of Villefranche-sur-Mer (a, b), Méjean (c, d) and Banyuls-sur-Mer (e, f) (see locations on Fig. 1). Isotherms every**  
 221  **$2.5^{\circ}\text{C}$ . The probe diagrams are smoothed vertically and over 24 hours in order to facilitate optimal viewing.**

222 In order to characterize southeasterly winds over the summer of 2022 in relation to climatology, statistics have been  
 223 compiled over the period 2012-2022. Each month, the time integral of negative WUDI (i.e. downwelling index) is  
 224 calculated. Figure A2 (Appendix A) shows the climatology of this index, the dispersion over 11 years and the value for  
 225 2022. Summer, and especially July and August, show very low values compared with autumn and winter, which also show  
 226 very high interannual variability. For the summer of 2022, downwelling dynamics is particularly weak in July, while in  
 227 August it is the strongest in the series, while remaining low compared to the rest of the year.

228  
 229 Figure 4 shows the surface wind fields during the two warmest events at depth (30 m), on August 13-14 and September 5-7.  
 230 In both cases, a low-pressure area was present over western Europe (western France in the first case, and the British Isles in  
 231 the second) leading to a southerly flow over the Mediterranean Sea, which penetrated the mainland in the Gulf of Lion. This  
 232 flow in the lower layers of the atmosphere was strongly influenced and accelerated by the relief especially by Corsica and  
 233 Sardinia, which were bypassed by veins of wind between and around the two islands. These wind veins converged in the  
 234 eastern Gulf of Lion, here influenced by the topography of the Provençal coast and the edge of the Alpine chain, producing a  
 235 noticeable acceleration in the vicinity of Marseille.



236  
 237 **Figure 4: ECMWF wind field ( $\text{m}\cdot\text{s}^{-1}$ ) at 10 m averaged over the two warmest subsurface periods: (a) 13-14 August 2022 ; (b) 5-7**  
 238 **September 2022. The black diamond stands for the Méjean observation point.**

### 239 4.3 Marine heatwaves

240 The warmest event at the surface and at 20 m at Méjean occurred in mid-August. At 30 and 40 m, temperatures peaked later  
241 in the season, during the September 6 event. Events were longest at the surface: the major event in mid-August lasted around  
242 2 weeks. While warm events were characterized by weak wind or moderate southeasterly wind conditions, they were  
243 stopped by northerly wind gusts along the northern coast (Fig. 2). The points discussed in the following 3 subsections are:  
244 warming during weak wind conditions (4.3.1), and during moderate southeasterly winds (4.3.2), and sensitivity of sub-  
245 surface warming to the duration of southeasterly winds (4.3.3).

#### 246 4.3.1 Case of weak winds: Impact of pre-existing upwelling

247 The upwellings that characterize the region studied here are mechanisms that a priori protect the coast from MHW by  
248 renewing surface water with deep cold water. However, Barrier et al. (2016) have highlighted a collateral effect that occurs  
249 when the upwelling stops, in the form of intrusions of the Northern Current on the Gulf of Lion shelf with a delay of 1 day  
250 after the wind relaxation. The impact of these intrusions on the occurrence of heatwaves in the eastern Gulf of Lion is  
251 described in this section.

252  
253 Five warming episodes were considered: June 13-18, July 9-12, August 1-4, August 8-12 and August 23-25, characterized  
254 by winds of less than  $5 \text{ m}\cdot\text{s}^{-1}$ , mostly blowing from the southeast, with occasional short spells from the northwest (Fig. 2).  
255 For each of these events, the temperature rise at 5 m ranged from 4 to  $7^\circ\text{C}$  (on average  $5.4^\circ\text{C}$ ). At 20 m, the warming was  
256 slightly lower ( $5^\circ\text{C}$  on average). It continued to decrease at 30 m ( $3^\circ\text{C}$  on average) and at 40 m ( $1.9^\circ\text{C}$  on average) (more  
257 details on the different events in Table A1 in Appendix A). The warming at 5 m cannot be due to a downwelling as this  
258 would imply a considerable temperature gradient between the surface and 5 m. Let's now consider the role of the solar  
259 radiation to explain this warming. For the July 9-12 event, the warming at 5 m was  $6.7^\circ\text{C}$  and  $5.4^\circ\text{C}$  at 20 m, in two days.  
260 The warming induced by the absorption of the heat associated to solar radiation, equal to  $320 \text{ W m}^{-2}$  on average over 24h, is  
261 around  $0.8^\circ\text{C}$ . Warming is therefore almost caused by a mechanism internal to the ocean. For each event considered, the  
262 warming at Méjean started between 1 and 3 days after the end of a northerly gale (varying in intensity from  $8$  to  $15 \text{ m}\cdot\text{s}^{-1}$ )  
263 and of the associated upwelling, which fits perfectly with the observations of Barrier et al. (2016) cited above. This process  
264 is responsible for the observed warming and it implies that the water mass advected during the Northern Current intrusion  
265 was much warmer than that present on the Gulf of Lion prior to the upwelling. The eastern part of the Gulf of Lion is  
266 particularly favorable to this situation, as it borders to the east of  $6^\circ\text{E}$ , an area much less exposed to northerly winds and  
267 therefore much more continuously warm at the surface (see the times series at Villefranche sur Mer in Fig. 3a).

268  
269 As an example, Fig. 5 a,b,c show the surface temperature and current for the second warming episode, on July 8, 12 and 15:  
270 at the peak of the northerly wind and upwelling on July 8, during and at the end of the warming phase on July 12 and 15,

271 respectively. The intrusion of a branch of the Northern Current advecting warm water is visible along the coast in the  
272 Marseille area after the stop of the northerly wind: the warm water mass was located east of 6°E on July 8 (Fig. 5a), then 50  
273 km further west on July 12 (Fig. 5b) and around 100 km (up to 5°E) on July 15. (Fig. 5c). It is also interesting to note that the  
274 strong, sustained northerly wind ( $\sim 10 \text{ m}\cdot\text{s}^{-1}$  for 4 days) which preceded the warming episode, produced marked hydrological  
275 structures (Fig. 5a) such as the upwelling front stretching southwards off Marseille and, further west, organized cross-shore  
276 currents. These structures, which persist for a few days, probably hinder the westward progress of warm waters.

277

#### 278 **4.3.2 Case of moderate to strong southeasterly winds**

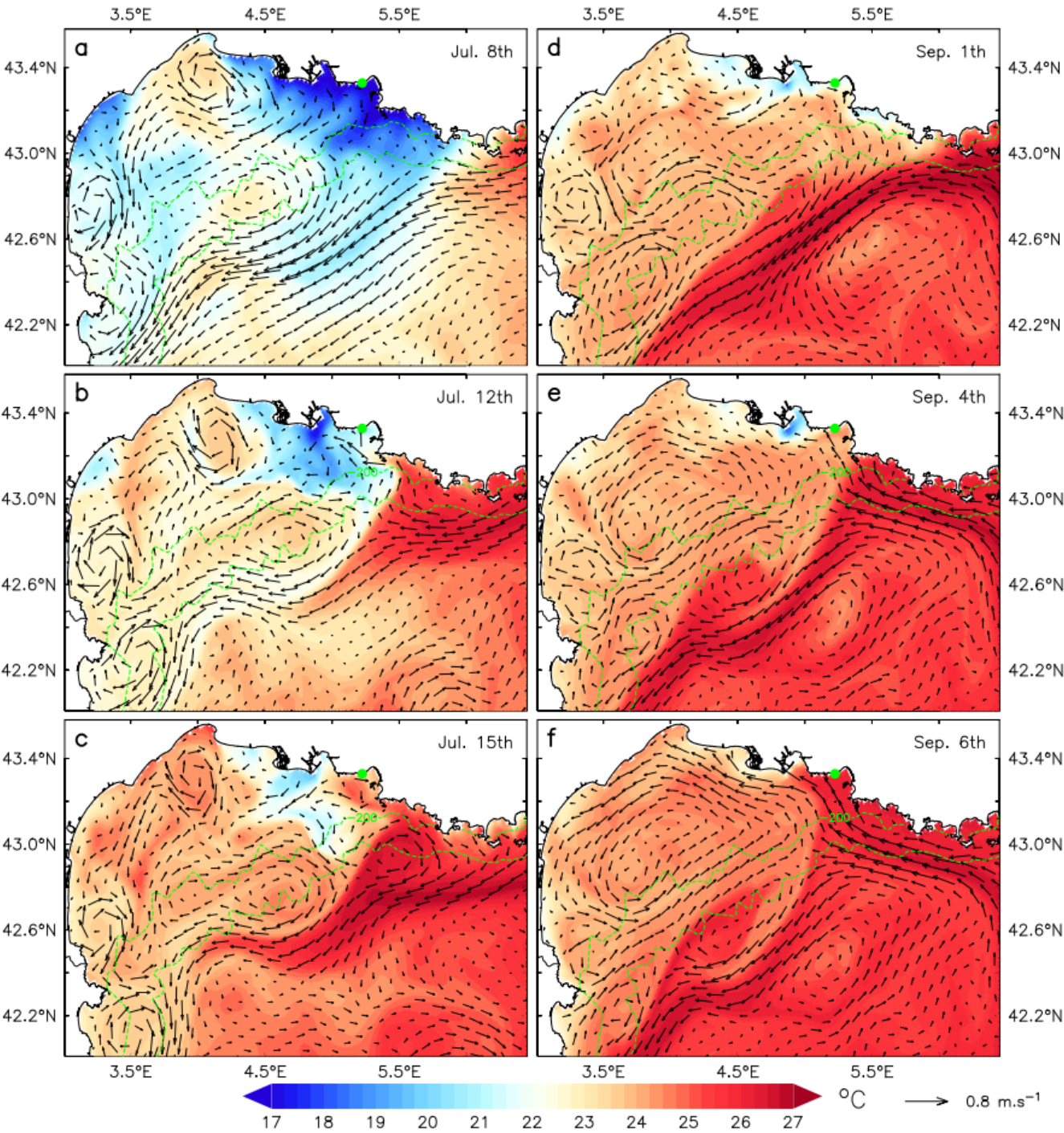
279 Odic et al. (2022) showed the tight correlations between downwelling favorable winds and 35 m temperature anomalies  
280 along the north-western Mediterranean shorelines. They quantified that the 75th percentile of the WUDI index for  
281 downwelling corresponded to an alongshore wind close to  $5 \text{ m}\cdot\text{s}^{-1}$  and a temperature response of  $+3 \text{ }^{\circ}\text{C}$  at 35 m for stratified  
282 conditions. Here, we examine the impact of such downwelling on subsurface heatwaves. According to Juza et al. (2022) and  
283 Darmaraki et al. (2024), such downwelling processes may indeed facilitate the vertical extension of heatwaves in the western  
284 Aegean and northeastern Crete.

285

286 We consider here the two cases associated with the warmest temperatures at 20 m: the August 12 to 14 event extended by a  
287 secondary peak on the 17th, and the September 2 to 7 event. In both cases, the southeasterly wind presented in Fig. 4,  
288 exceeded  $8 \text{ m}\cdot\text{s}^{-1}$  and the WUDI index fell, showing coastward transports of over  $0.5 \text{ m}^3\cdot\text{s}^{-1}\cdot(\text{coastline m})^{-1}$  that lasted 2 days  
289 (Fig. 2). The vertical distribution of warming was quite different from that of low winds (Fig. 2, Table A1 & Fig. 3) :  
290 warming was minimal at the surface, as temperatures were already high at the start of both events, and increased down to 30  
291 m, with values of  $5.5 \text{ }^{\circ}\text{C}$  in August and  $8.8 \text{ }^{\circ}\text{C}$  in September (compared with  $2\text{-}3.6 \text{ }^{\circ}\text{C}$  for weak winds). At 40 m, warming  
292 was  $2 \text{ }^{\circ}\text{C}$  for the first (and shorter) event, and  $8.5 \text{ }^{\circ}\text{C}$  for the second one. Again in contrast to the low-wind cases, the  
293 northerly wind preceding the September 6 event was weak (less than  $10 \text{ m}\cdot\text{s}^{-1}$ ) and of short duration (from August 31 to  
294 September 1) and as a result, the associated upwelling (Fig. 5d) and the currents on the inner shelf were poorly developed,  
295 and the intrusion of the Northern Current associated with the cessation of upwelling was weak. The warming during this  
296 event was therefore rather related to the southeasterly wind causing surface water to pile up against the coast, inducing the  
297 downwelling of warm surface water, and finally, through geostrophy, the development of an alongshore westward jet. The  
298 persistence of the easterly wind (6 days without interruption) and the weak currents that prevailed before, favored the  
299 establishment of this alongshore circulation at the whole continental shelf scale, warming a large part of the coastal zone of  
300 the Gulf of Lion between September 1 and 6, as shown in Fig. 5f. At a depth of 30 m, Fig. 6a-c show the pre-event and peak  
301 temperatures and their differences, indicating that the eastern Gulf of Lion was warmed up by around  $7^{\circ}\text{C}$  over  $600 \text{ km}^2$  from  
302  $5.62^{\circ}\text{E}$  east of Cassis to  $4.85^{\circ}\text{E}$  near the Rhône mouth. Further west, the coastal strip extending up to the 60 m isobath was



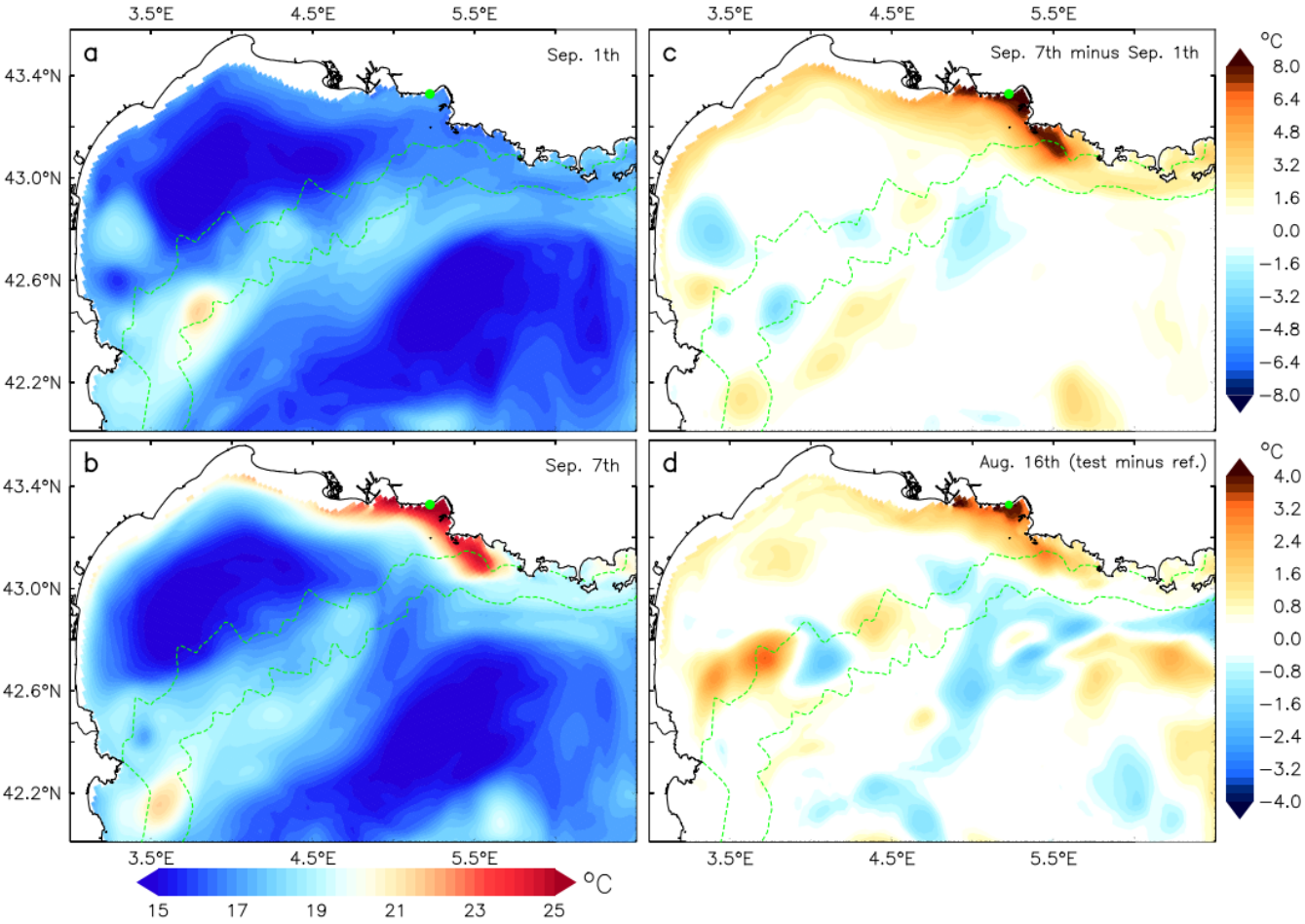
303 heated by 2 to 4 °C. The similarity between the area of maximum warming and that of maximum downwelling favorable  
304 winds (Fig. 4b) is remarkable.



305

25  
26

306 **Figure 5: Surface temperature (°C) and current simulated for the surface warming event of July (a,b,c) : (a) July 8 (during the**  
 307 **upwelling), (b) July 12 (the day after the wind stopped), (c) July 15. Same for the subsurface warming event of September (d,e,f):**  
 308 **(d) September 1, (e) September 4, (f) September 6. The green point stands for the Méjean TMED-Net observation point. The green**  
 309 **dashed lines are the 200 and 1000 m isobaths.**



310  
 311 **Figure 6: (a-c): September event. Temperature (°C) at 30 m depth before the September subsurface warming event (a : September**  
 312 **1) and at the peak of the event (b: September 7); (c) warming between these two dates; (d) August event. Temperature difference**  
 313 **(°C) at 30 m depth on August 16 between the test (extension of the southeasterly wind period) and the reference simulations. The**  
 314 **green dashed lines are the 200 and 1000 m isobaths.**

### 315 4.3.3 Sensitivity of heat penetration in depth to the duration of the southeasterly wind

316 We consider the mid-August event at Méjean, the warmest of the summer at the surface. We described it as a succession of  
 317 two main events (Fig. 2e-f) : one with weak winds from August 8 to 12, and the second with sustained southeasterly winds  
 318 from August 12 to 14 (Fig. 4a), when sponge mortality in the Bay of Marseille began to be observed. This mortality was  
 319 massively concentrated in the 0-25 m layer and more sparsely at 30 m. The second event is not detailed because it is similar  
 320 to the one in September, except that, as mentioned in the previous paragraph, the duration of the southeasterly wind was

shorter and the deep warming was lower in August. To understand the relation between warming and the duration of the southeasterly wind, we conducted a sensitivity study to this duration. The sustained wind event lasted about 40 hours. As the occurrence of southeasterly winds is high in August 2022 (fig. A2), we limit the extension of the southeasterly wind period by one day. This modification was made during the weakening wind period from 1 PM on August 14 to 1 PM on August 15, where we substituted the stronger wind from the period of 1 AM on August 13 to 1 AM on August 14. The temperature at 30 m of the reference simulation being underestimated from August 15 to 18 by 3 °C on average (Fig. 2), we will subsequently present differences between the test and the reference simulations rather than the biased warming for each simulation. Figure 6d represents this temperature difference at 30 m on August 16. As expected, the lengthening of the period of southeasterly winds results in increased warming. The temperature difference at 30 m from August 15 to 17 exceeds 3.5 °C around Marseille. The daily average temperature observed on August 14 and 15 was 23.8 °C. If we transpose the results of the sensitivity test to the observed series, we deduce that the temperature at 30 m would have reached the value at 20 m. This would likely have led to a deepening of the mass mortality zone to 30 m instead of 25 m, and partial mortality at 35 m due to an increased warming of 1.3 °C compared to the reference simulation. It can be seen that the maximum warming along the Gulf of Lion coast is in the same place as in the early September situation (Fig. 6c). This is also where the southeasterly wind is strongest during the warming period (Fig. 4a).

#### 4.4 Impact on marine benthic communities

Under the influence of southeasterly wind regimes, which induced warm water downwelling to a depth of 30 m, and MHWs that exhibited heightened intensity across a 600 km<sup>2</sup> area between 5.62 °E (east of Cassis) and 4.85 °E (near the Rhône River mouth), gorgonian mortality was observed to be both more severe and extended to greater depths within this region. Generally speaking, the impact on gorgonian populations appears to be most severe in the “Cap Sicié”, “Parc National des Calanques”, and “Parc Marin de la Côte Bleue” areas, particularly for the red gorgonian (*P. clavata*). For this species, which is the most sensitive, more than 50% of the populations monitored in the 20 to 30 m depth range in the PnCal showed a severe impact (> 60% of affected colonies), compared with less than 10% in Port Cros for the same depth range (Fig. 7). More specifically, in line with the MHWs observed, no impact has been recorded for the *E. cavolini* in the PNPC area, while a sometimes severe impact has been recorded for this species in the PnCal and PMCB areas. The same observation was made for *E. singularis*, whose populations were less affected (10-30% affected colonies) in the PNPC area for the 10-20 m depth range and were not affected deeper, while the populations were sometimes severely affected (> 60% of affected colonies) down to 20 m in the PnCal area, and moderately affected (30-60% of affected colonies) in the PMCB down to 30 m. These observations suggest a greater impact at greater depths (down to 30m) for the gorgonian populations around the Marseille region than within the PNPC.

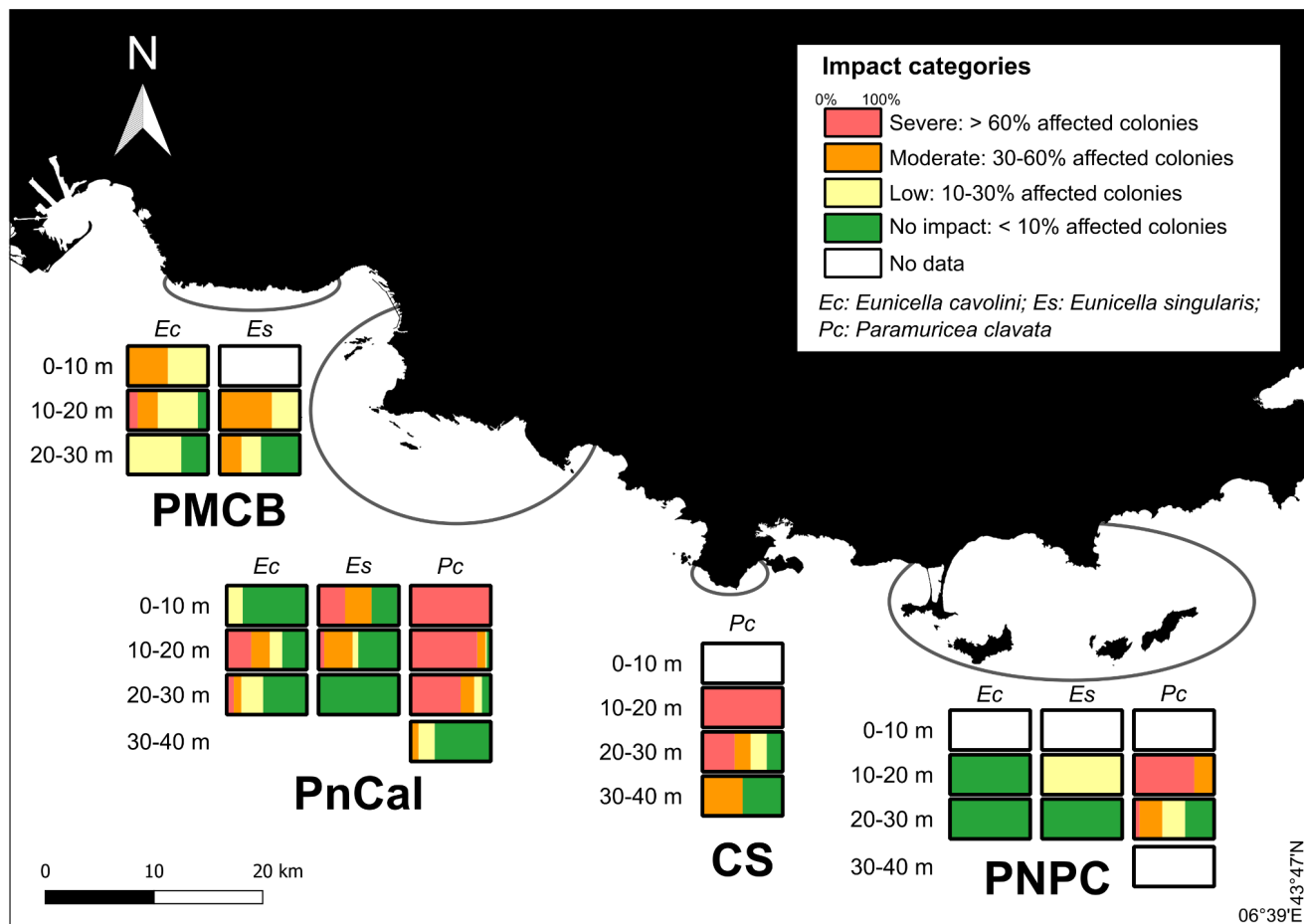


**Figure 7: Map showing the severity of the impact of the mass mortality event on the gorgonian populations of the “Parc Marin de la Côte Bleue” (PMCB), the “Parc National des Calanques” (PnCal), the “Cap Sicié” (CS), and the “Parc National de Port-Cros” (PNPC). The impact on populations is represented by 10 m depth ranges between the surface and 40 m. See Estaque et al. (2023) for more details on the monitoring method. Data for *P. clavata* in the PnCal are presented in more detail in Estaque et al. (2023).**

#### 4.5 Variability of deep heatwaves on a regional scale

Figure 3 illustrates the major spatial variability of the upper layers temperature chronology on a regional scale. The upwelling and downwelling temperature alternations discussed at Méjean are much reduced at the other two sites. Villefranche-sur-Mer is characterized by the presence of warm water throughout the summer in the surface layer, due to warming by the Northern Current flowing close to the coast and weak winds. Surface temperatures are frequently as high as the maximum recorded at Méjean on August 15. The two deep heatwave events studied at Méjean are also present at Villefranche-sur-Mer, also indicating the influence of the easterly wind in this region, albeit attenuated compared with the Marseille area (Fig. 3), which reduces the depth impacted by downwelling by about 10 m. At Banyuls-sur-Mer, the situation is different from the two other sites, with repeated temperature peaks almost reaching 40 m. The deep heatwave events of mid-August and early September studied at Mejean are also present, albeit a few days late but temperature peaks are lower



366 than at the two other sites, reflecting the reduced influence of the Northern Current over most of the Gulf of Lion shelf and  
367 the frequent presence of dry northerly winds cooling the surface.

## 368 **5. Discussion and perspectives**

369 During the summer of 2022, the atmospheric heatwaves that hit Western Europe gave rise to extreme marine heatwaves  
370 across the western Mediterranean as shown by Guinaldo et al. (2023). Although being a coastal zone relatively tempered by  
371 the recurrence of northerly winds and associated upwelling, the east of the Gulf of Lion and the very rich benthic ecosystems  
372 that it shelters have been exposed to short periods of exceptional temperatures.

373

374 The succession of hot and cold events in summer 2022 has been successfully reproduced by a numerical simulation: all  
375 events have been simulated and the correlations are generally above 0.9. To go further, the precise reproduction of warm  
376 events is a major issue when it comes to determining the crossing of thermal thresholds representing the survival of marine  
377 species. In order to improve this precision, we identify two sensitive points here. On the one hand, a higher resolution of the  
378 horizontal grid will improve the description of the strong bathymetric gradients characteristic of the coastal area around  
379 Marseille and further east, along the Ligurian coast, and consequently the representation of horizontal and vertical  
380 movements. On the other hand, the accuracy of the near-shore wind field is likely crucial for the accuracy of simulated  
381 temperatures due to the influence of topography on wind channeling and acceleration. Exploring the uncertainties of these  
382 two origins would be informative to improve the description of risk areas and to be able to predict extreme temperatures with  
383 better precision without unnecessarily increasing computational costs.

384

385 Despite the uncertainties, our modeling results provide insights into the two types of heatwaves that were recorded in 2022.  
386 The first type of heatwave is a surface phenomenon. The physical processes at play are recurrent when the northerly winds  
387 and induced upwelling stop, and the wind speed following the northerly wind is less than  $\sim 5 \text{ m}\cdot\text{s}^{-1}$ . This succession of  
388 meteorological conditions causes an intrusion of warm water from the Northern Current along the northeast coast of the Gulf  
389 of Lion. In these situations, only the 5 m level exceeded 25 °C. In summary, these events renew the coastal water mass by an  
390 advection of warm water until the following northerly gale which replaces the surface water with cold subsurface water. The  
391 second type of heatwave, more dramatic because it affected depths of 30 to 40 m, is generated by southeasterly winds  
392 (around  $8 - 10 \text{ m}\cdot\text{s}^{-1}$ ). Surface heating is still due to the advection of warm water from the east but it is pushed downward by  
393 wind-induced coastal downwelling. The strength and duration of the southeasterly wind are crucial parameters which  
394 determine the depth impacted. This second type of events marked by pronounced sub-surface heatwaves induced by  
395 downwelling was highlighted by Juza et al. (2022) and Darmaraki et al. (2024) in other Mediterranean regions.

396

397 On a regional scale ( $\sim 200$  km), we have shown considerable variability in surface and deep heatwaves for two reasons: (i)  
398 the channeling of northerly and easterly winds by the continental relief associated with the complex shape of the coastline,  
399 which produces localized upwelling and downwelling, and (ii) warming by the Northern Current, whose influence is great  
400 along the Ligurian coast and reduced in the western part of the Gulf of Lion. This high spatio-temporal variability of  
401 heatwaves in coastal areas contrasts with heatwaves in open seas, which are much more widespread and also more spatially  
402 homogeneous. TMED-Net network is an extremely valuable tool for documenting this variability and providing a database  
403 for validating high-resolution numerical models.

404

405 The severity of the 2022 summer for benthic species is the result of the superposition of two conditions, both exceptional,  
406 which are (1) the atmospheric heatwave which led to an exceptional warming of the surface of the western Mediterranean  
407 Sea and (2) the two southeasterly wind events in mid-August and early September which caused these warm waters to  
408 plunge to depth. These latter events are rare in summer as evidenced by the monthly downwelling index which is the highest  
409 in the decade for August, to which must be added the major event that occurs at the beginning of September. The occurrence  
410 of sustained southeasterly winds in summer, when surface temperatures are warmest, therefore constitutes a major danger for  
411 coastal ecosystems particularly for benthic species located above 40 m depth. The coastal region around 30 km on either side  
412 of Marseille, with its remarkable habitats, is at far greater risk than the rest of the Gulf of Lion, due to the acceleration of  
413 southeasterly winds caused by the topography, which locally intensifies downwelling. Indeed, we have verified that the  
414 acceleration shown here for the two major events of August and September 2022 exists in most of southeasterly wind  
415 situations occurring between June and September over the period 2012-2022. This is indirectly confirmed by Odic et al  
416 (2022) who, using the wind from the ERA5 reanalysis to calculate upwelling and downwelling indices, showed that the  
417 Marseille vicinity is not only the most powerful upwelling zone in the northern Gulf of Lion, but also the most exposed to  
418 downwelling.

419

420 Global warming was proven to have contributed to the extreme temperatures experienced in the western Mediterranean Sea  
421 during the summer of 2022 (Faranda et al., 2023). Exploring the coincidence of southeasterly winds and surface heatwaves  
422 in future climate scenarios would help anticipate the recurrence of massive mortality events and ultimately the disappearance  
423 of benthic populations, which are emblematic of the Calanques region of Marseille and of the Côte Bleue. Given the ongoing  
424 global warming trends, an increase in the frequency and intensity of MHWs in the affected depth zones (0 - 30 m) and  
425 deeper is expected. These extreme thermal events are likely to severely impact the potential recovery of benthic organism  
426 populations, and the potential role of refuge from deeper populations is not certain (Bramanti et al., 2023). Certain benthic  
427 species, such as gorgonians, play a crucial role as ecosystem engineers, contributing significantly to habitat complexity  
428 (Verdura et al., 2019). The collapse of these species would therefore lead to a marked reduction in structural diversity, with  
429 cascading effects on the broader ecosystem, including the disruption of ecological functions (Ponti et al., 2014) and the loss  
430 of vital ecosystem services (Estaque et al., 2023; Garrabou et al., 2021; Gómez-Gras et al., 2021). To mitigate these impacts,

431 it is imperative to adopt multidisciplinary approaches that integrate ecological, oceanographic, and climatological data to  
432 better predict the occurrence and intensity of MHWs. Such strategies are essential for developing adaptive coastal area  
433 management and conservation efforts, with the goal of preserving the integrity of Mediterranean benthic communities and  
434 maintaining the ecosystem services they provide. In a context where management plans are predominantly designed within a  
435 two-dimensional framework (Jacquemond et al., 2024), this approach marks a critical advancement towards recognizing the  
436 ocean as a three-dimensional environment, particularly when establishing marine protected areas and conservation zones.  
437  
438 Finally, heatwaves will not only intensify in frequency and intensity with climate change but thermal stress will combine  
439 with other stresses whether linked to the long-term increase in anthropogenic CO<sub>2</sub> or to the short-term impact of heatwaves  
440 on the chemical and biogeochemical composition of water. An extension of this study towards the impact of the 2022  
441 heatwaves on oxygen, pH and chlorophyll concentrations in the Gulf of Lion is planned.  
442

443    **Appendix A**

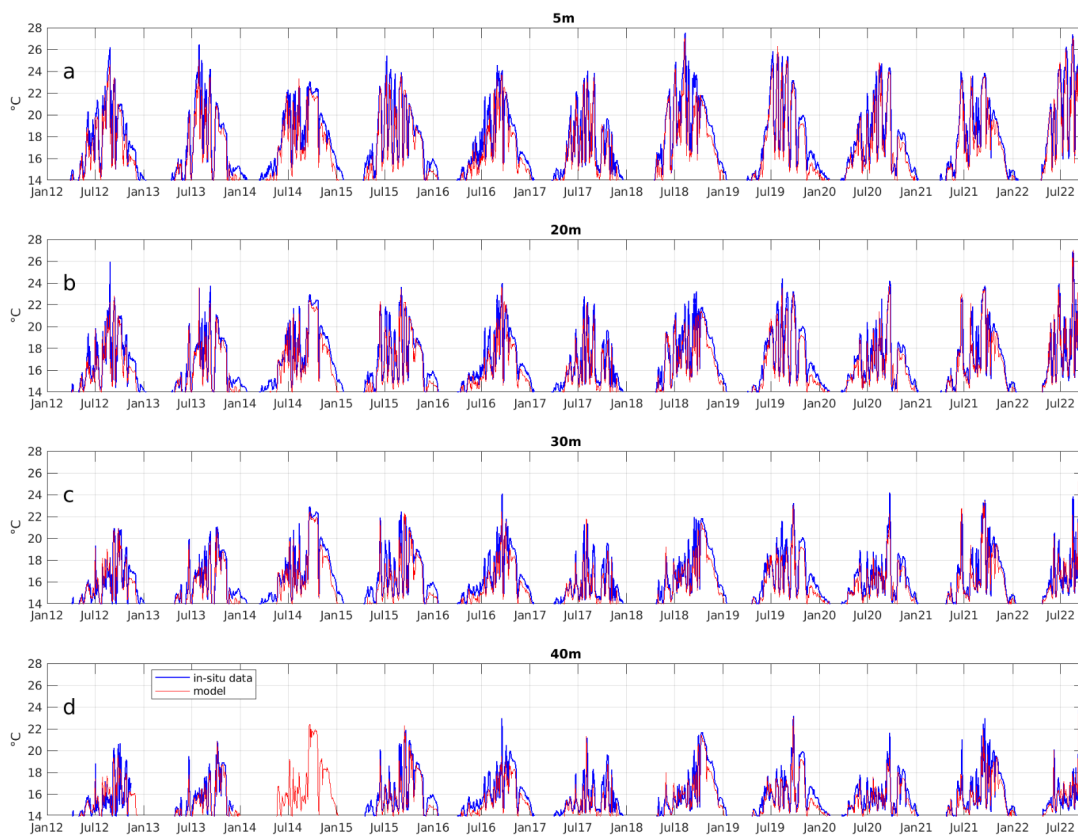
<b>Surface event</b>	<b>5 m warming</b>	<b>20 m warming</b>	<b>30 m warming</b>	<b>40 m warming</b>
June 13-18	4.8	4.2	2.3	1.8
July 9-12	6.7	5.4	2.6	1.4
August 1-4	4.1	4.7	3.6	2.
August 8-12	4.7	4.2	2.	1.1
August 23-25	6.8	6.4	4.8	3.
<b><i>Average</i></b>	<b><i>5.4</i></b>	<b><i>5.</i></b>	<b><i>3.</i></b>	<b><i>1.9</i></b>
<b>Subsurface event</b>	<b>5 m warming</b>	<b>20 m warming</b>	<b>30 m warming</b>	<b>40 m warming</b>
August 12-14	0.6	5.6	5.8	1.9
September 2-7	2.1	7.5	8.8	8.5
<b><i>Average</i></b>	<b><i>1.4</i></b>	<b><i>6.5</i></b>	<b><i>7.3</i></b>	<b><i>5.2</i></b>

444

445    **Table A1: Identification of the different surface and subsurface warm events. Warming in °C observed at Méjean over each period**  
446    **at different depths (TMED-Net data).**

447

448



449

450

451

452

**Figure A1: Observed (blue) and simulated (red) temperature time series at the Méjean station of the TMED-Net network from 2012 to 2022 from 5 m to 40 m as indicated above the figures. The frequency shown is daily. Note the absence of in-situ data in 2014 at 40 m due to technical problems.**

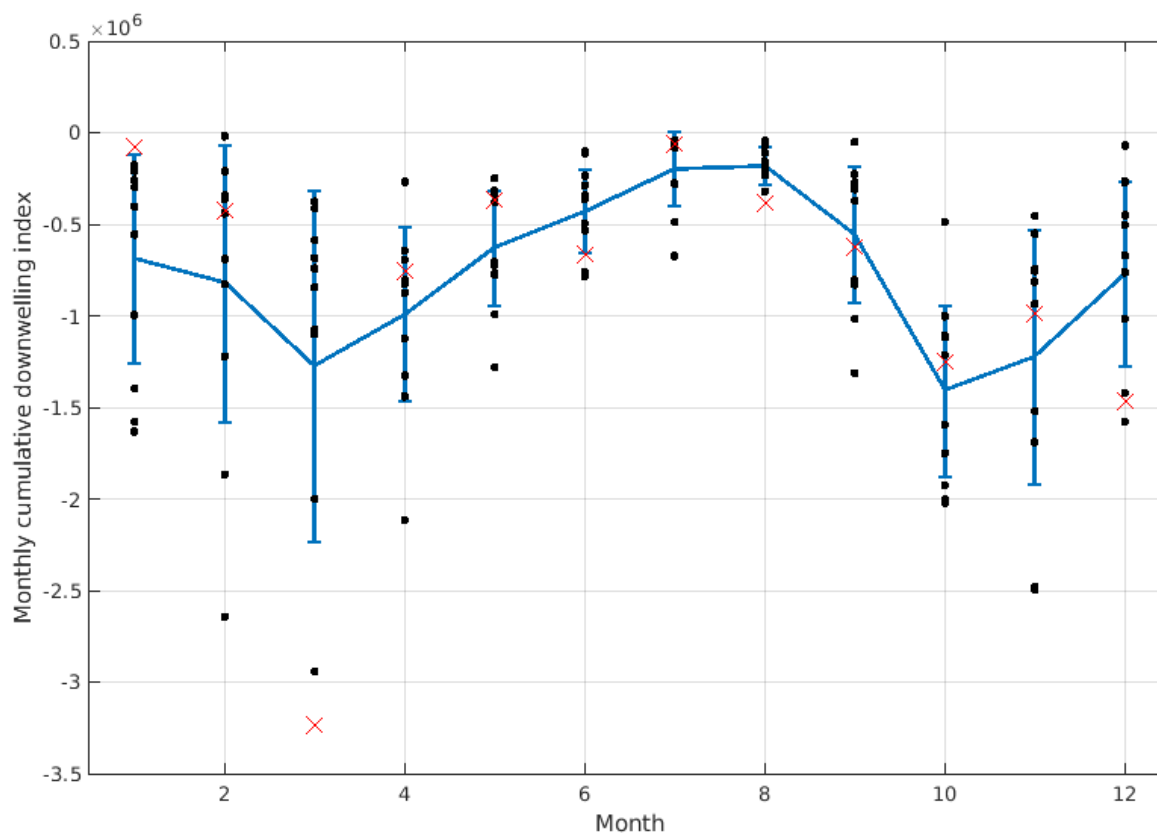


**Figure A2: Monthly cumulative downwelling index ( $\text{m}^3 \cdot (\text{coastline m})^{-1}$ ) off Marseille. Blue curve: climatology  $\pm$  standard deviation calculated over 2012-2022. Black dots represent the monthly values for each year and the red cross is for 2022.**

## Author contribution

CU and CE planned the study and conceptualized the paper. TE analysed the biological data. The model was developed by PM. CE and PM performed the simulations. QBB analysed the meteorological forcing. CE and TE wrote the first version of the paper. All co-authors edited and corrected the text.

## Competing interests

The authors declare that they have no conflict of interest.

## Acknowledgments

This study was funded by the OFB (Office français de la biodiversité) and ILICO littoral and coastal research infrastructure ([www.ir-ilico.fr](http://www.ir-ilico.fr)) through the INTEGRATION workshop for the study of marine heatwaves along the French coastline. The

temperature in-situ data have been provided by the regional temperature observation network T-MEDNet, [www.t-mednet.org](http://www.t-mednet.org), site "Méjean", Dorian Guillemain, OSU Institut Pythéas, site "Villefranche-sur-Mer", Nuria Teixido and Steeve Comeau, Laboratoire d'Océanographie de Villefranche-su-Mer, site "Banyuls-sur-Mer", Ronan Rivoal, Réserve Naturelle Marine de Cerbère Banyuls /Conseil Départemental des Pyrénées Orientales. For the health data on gorgonian populations, we would like to thank Eric Charbonnel, Patrick Bonhomme, Pauline Vouriot, Stéphane Sartoretto, Quentin Schull, Bastien Mérigot and the entire Septentrion Environnement team. The SYMPHONIE model and the simulations produced are distributed by the national service SIROCCO (<https://sirocco.obs-mip.fr>) of CNRS-INSU coordinated by the ILICO research infrastructure. The simulations were performed using HPC resources from CALMIP (Grant P09115). CE is grateful to Pierre Chevaldonné and Thierry Perez for their constructive feedback.

## References

- Barrier, N., Petrenko, A.A., and Ourmières, Y.: Strong intrusions of the Northern Mediterranean Current on the eastern Gulf of Lion: insights from in-situ observations and high resolution numerical modelling. *Ocean Dynamics* 66, 313–327, 2016. doi:10.1007/s10236-016-0921-7
- Bensoussan, N., Romano, J. C., Harmelin, J. G., and Garrabou, J.: High resolution characterization of Northwest Mediterranean coastal waters thermal regimes: To better understand responses of benthic communities to climate change. *Estuarine Coastal Shelf Science*, 87, 431–441. doi:10.1016/j.ecss.2010.01.008, 2010.
- Bramanti, L., Manea, E., Giordano, B., Estaque, T., Bianchimani, O., Richaume, J., Mérigot, B., Schull, Q., Sartoretto, S., Garrabou, J. G., & Guizien, K.: The deep vault: a temporary refuge for temperate gorgonian forests facing marine heat waves. *Mediterranean Marine Science*, 24(3), 601–609, doi:10.12681/mms.35564, 2023.
- Crisci, C., Bensoussan, N., Romano, J.-C., and Garrabou, J.: Temperature anomalies and mortality events in marine communities: Insights on factors behind differential mortality impacts in the NW Mediterranean. *PLoS One*, 6(9), e23814, doi:10.1371/journal.pone.0023814, 2011.
- Damien, P., Bosse, A., Testor, P., Marsaleix, P., Estournel, C.: Modeling post-convective submesoscale coherent vortices in the northwestern Mediterranean Sea. *J. Geophys. Res. Oceans*, doi:10.1002/2016JC012114, 2017.
- Darmaraki, S., Denaxa, D., Theodorou, I., Livanou, E., Rigatou, D., Raitsos E.D., Stavrakidis-Zachou, O., Dimarchopoulou D., Bonino, G., McAdam, R., Organelli, E., Pitsouni, A., & Parasyris, A. (2024). Marine Heatwaves in the Mediterranean Sea: A Literature Review. *Mediterranean Marine Science*, 25(3), 586–620. <https://doi.org/10.12681/mms.38392>
- Drobinski, P., and Coauthors: HyMeX: A 10-Year Multidisciplinary Program on the Mediterranean Water Cycle. *Bull. Amer. Meteor. Soc.*, 95, 1063–1082, doi:10.1175/BAMS-D-12-00242.1, 2014.
- Ducrocq, V., and Coauthors: HyMeX-SOP1: The Field Campaign Dedicated to Heavy Precipitation and Flash Flooding in the Northwestern Mediterranean. *Bull. Amer. Meteor. Soc.*, 95, 1083–1100, doi: 10.1175/BAMS-D-12-00244.1, 2014.

497 Estaque, T., Richaume, J., Bianchimani, O., et al.: Marine heatwaves on the rise: One of the strongest ever observed mass  
498 mortality event in temperate gorgonians. *Global Change Biology*. 29(22):6159-6162, doi:10.1111/gcb.16931, 2023.

499 Estournel, C., Testor, P., Damien, P., D’Ortenzio, F., Marsaleix, P., Conan, P., Kessouri, F., Durrieu de Madron, X.,  
500 Coppola, L., Lellouche, J.M., Belamari, S., Mortier, L., Ulses, C., Bouin, M.N., Prieur, L. : High resolution modeling of  
501 dense water formation in the north-western Mediterranean during winter 2012–2013: Processes and budget. *Journal of*  
502 *Geophysical Research – Oceans*, doi:10.1002/2016JC011935, 2016.

503 Estournel, C., Marsaleix, P. and Ulses, C.: A new assessment of the circulation of Atlantic and Intermediate Waters in the  
504 Eastern Mediterranean. *Progress in Oceanography*, 198, 102673, doi:10.1016/j.pocean.2021.102673, 2021.

505 Faranda, D., Pascale, S., Bulut, B.: Persistent anticyclonic conditions and climate change exacerbated the exceptional 2022  
506 European-Mediterranean drought. *Environ. Res. Lett.*, 18 034030, doi:10.1088/1748-9326/acbc37, 2023.

507 Fox-Kemper, B., H.T. Hewitt, C. Xiao, G. Aðalgeirsdóttir, S.S. Drijfhout, T.L. Edwards, N.R. Golledge, M. Hemer, R.E.  
508 Kopp, G. Krinner, A. Mix, D. Notz, S. Nowicki, I.S. Nurhati, L. Ruiz, J.-B. Sallée, A.B.A. Slangen, and Y. Yu: Ocean,  
509 Cryosphere and Sea Level Change. In *Climate Change 2021: The Physical Science Basis. Contribution of Working Group I*  
510 *to the Sixth Assessment Report of the Intergovernmental Panel on Climate Change* [Masson-Delmotte, V., P. Zhai, A. Pirani,  
511 S.L. Connors, C. Péan, S. Berger, N. Caud, Y. Chen, L. Goldfarb, M.I. Gomis, M. Huang, K. Leitzell, E. Lonnoy, J.B.R.  
512 Matthews, T.K. Maycock, T. Waterfield, O. Yelekçi, R. Yu, and B. Zhou (eds.)]. Cambridge University Press, Cambridge,  
513 United Kingdom and New York, NY, USA, pp. 1211–1362, doi:10.1017/9781009157896.011, 2021.

514 Garrabou, J., Ledoux, J.B., Bensoussan, N., Gómez-Gras, D., Linares, C.: Sliding Toward the Collapse of Mediterranean  
515 Coastal Marine Rocky Ecosystems. In: Canadell, J.G., Jackson, R.B. (eds) *Ecosystem Collapse and Climate Change*.  
516 *Ecological Studies*, vol 241. Springer, Cham., doi:10.1007/978-3-030-71330-0\_11, 2021.

517 Garrabou, J., Gómez-Gras, D., Medrano, A., Cerrano, C., Ponti, M., Schlegel, R., Bensoussan, N., Turicchia, E., Sini, M.,  
518 Gerovasileiou, V., Teixido, N., Mirasole, A., Tamburello, L., Cebrian, E., Rilov, G., Ledoux, J.-B., Souissi, J. B., Khamassi,  
519 F., Ghanem, R. ... Harmelin, J.-G.: Marine heatwaves drive recurrent mass mortalities in the Mediterranean Sea. *Global*  
520 *Change Biology*, 28, 5708–5725, doi:10.1111/gcb.16301, 2022.

521 Gómez-Gras D., Linares C., López-Sanz A., Amate R., Ledoux J. B., Bensoussan N., Drap P., Bianchimani O., Marschal C.,  
522 Torrents O., Zuberer F., Cebrian E., Teixidó N., Zabala M., Kipson S., Kersting D. K., Montero-Serra I., Pagès-Escalà M.,  
523 Medrano A., Frleta-Valić M., Dimarchopoulou D., López-Sendino P. and Garrabou J.: Population collapse of habitat-  
524 forming species in the Mediterranean: a long-term study of gorgonian populations affected by recurrent marine heatwaves.  
525 *Proc. R. Soc. B.*, 28820212384, doi:10.1098/rspb.2021.2384, 2021.

526 Grenier, M., Idan, T., Chevaldonné, P., Perez, T.: Mediterranean marine keystone species on the brink of extinction. *Glob.*  
527 *Change Biol.*, 29, 1681-1683, doi:10.1111/gcb.16597, 2023.

528 Guinaldo, T., Voldoire, A., Waldman, R., Saux Picart, S., and Roquet, H.: Response of the sea surface temperature to  
529 heatwaves during the France 2022 meteorological summer. *Ocean Sci.*, 19, 629–647, doi:10.5194/os-19-629-2023, 2023.



530 Glynn, P.W., D'Croz, L. : Experimental evidence for high temperature stress as the cause of El Niño coincident coral  
531 mortality. *Coral Reefs*, 8, 181-191, doi:10.1007/BF00265009, 1990.

532 Hughes, T., Kerry, J., Álvarez-Noriega, M. et al.: Global warming and recurrent mass bleaching of corals. *Nature*, 543, 373–  
533 377, doi:10.1038/nature21707, 2017.

534 Jacquemont, J., Loiseau, C., Tornabene, L. et al.: 3D ocean assessments reveal that fisheries reach deep but marine  
535 protection remains shallow. *Nat. Commun.*, 15, 4027, doi:10.1038/s41467-024-47975-1, 2024.

536 Juza, M, Fernández-Mora, À, Tintoré, J.: Sub-Regional Marine Heat Waves in the Mediterranean Sea From Observations:  
537 Long-Term Surface Changes, Sub-Surface and Coastal Responses. *Front. Mar. Sci.*, 9:785771,  
538 doi:10.3389/fmars.2022.785771, 2022.

539 Lejeusne, C., Chevaldonné, P., • Pergent-Martini, C., • Boudouresque, C.F., • Pérez, T. : Climate change  
540 effects on a miniature ocean: the highly diverse, highly impacted Mediterranean Sea. *Trends in Ecology & Evolution*, 25, 4,  
541 250 – 260,doi: 10.1016/j.tree.2009.10.009, 2010.

542 Marsaleix, P., Auclair, F., Estournel, C.: Considerations on Open Boundary Conditions for Regional and Coastal Ocean  
543 Models. *Journal of Atmospheric and Oceanic Technology*, 23,1604-1613, doi: 10.1175/JTECH1930.1, 2006.

544 Marsaleix, P., Auclair, F., Floor, J. W., Herrmann, M. J., Estournel, C., Pairaud, I., Ulses, C.: Energy conservation issues in  
545 sigma-coordinate free-surface ocean models. *Ocean Modelling*, 20, 61-89, doi:10.1016/j.ocemod.2007.07.005,2008.

546 Martinez, J., Leonelli, F.E., Garcia-Ladona, E., Garrabou, J., Kersting, D.K., Bensoussan, N. and Pisano, A.: Evolution of  
547 marine heatwaves in warming seas: the Mediterranean Sea case study. *Front. Mar. Sci.*, 10:1193164,  
548 doi:10.3389/fmars.2023.1193164, 2023.

549 Marullo S., et al.: Record-breaking persistence of the 2022/23 marine heatwave in the Mediterranean Sea. *Environ. Res.*  
550 *Lett.* ,18, 114041, doi:10.1088/1748-9326/ad02ae, 2023.

551 Mikolajczak, G., Ulses, C., Estournel, C., Bourrin, F., Pairaud, I., Martín, J., Puig, P., Durrieu de Madron, X., Leredde, Y.,  
552 Marsaleix, P. : Impact of storms on residence times and export of coastal waters during a mild fall/winter period in the Gulf  
553 of Lion. *Continental Shelf Research*, 207, 104192, doi:10.1016/j.csr.2020.104192, 2020.

554 Millot, C.: The gulf of Lions' hydrodynamics. *Continental Shelf Research*, 10, 9-11, 885-894, 1990.

555 Obermann-Hellhund, A., Conte, D., Somot, S. et al.: Mistral and Tramontane wind systems in climate simulations from  
556 1950 to 2100. *Clim. Dyn.*, 50, 693–703, doi:10.1007/s00382-017-3635-8, 2018.

557 Odic, R., Bensoussan, N., Pinazo, C., Taupier-Letage, I., Rossi, V.: Sporadic wind-driven upwelling / downwelling and  
558 associated cooling / warming along Northwestern Mediterranean coastlines. *Continental Shelf Research*, 250, 104843,  
559 doi:10.1016/j.csr.2022.104843, 2022.

560 Pairaud, I.L., Bensoussan, N., Garreau, P. et al.: Impacts of climate change on coastal benthic ecosystems: assessing the  
561 current risk of mortality outbreaks associated with thermal stress in NW Mediterranean coastal areas. *Ocean Dynamics*, 64,  
562 103–115, doi:10.1007/s10236-013-0661-x, 2014.

563 Pastor, F., Valiente, J.A., Khodayar, S.: A Warming Mediterranean: 38 Years of Increasing Sea Surface Temperature.  
564 Remote Sens., 12, 2687, doi:10.3390/rs12172687, 2020.

565 Pastor, F. & Khodayar Pardo, S.: Marine heat waves: Characterizing a major climate impact in the Mediterranean. Science of  
566 The Total Environment, 861, 160621, doi:10.1016/j.scitotenv.2022.160621, 2023.

567 Ponti, M., Perlini R.A., Ventra V., Grech D., Abbiati M., Cerrano C.: Ecological Shifts in Mediterranean Coralligenous  
568 Assemblages Related to Gorgonian Forest Loss. PLoS ONE 9(7): e102782, doi:10.1371/journal.pone.0102782, 2014.

569 Ross, O.N., Fraysse, M., Pinazo, C., Pairaud, I.: Impact of an intrusion by the Northern Current on the biogeochemistry in  
570 the eastern Gulf of Lion, NW Mediterranean. Estuarine, Coastal and Shelf Science, 170, 1-9, doi:10.1016/j.ecss.2015.12.022,  
571 2016.

572 Sartoretto, S., Ledoux J.B., Gueret E., Guillemain D., Ravel C., Moirand L., Aurelle D.: Ecological and genomic  
573 characterization of a remarkable natural heritage: a mesophotic ‘giant’ *Paramuricea clavata* forest. Mar. Ecol. Prog. Ser.,  
574 728:85-101, doi:10.3354/meps14427, 2023.

575 Schaeffer, A., Sen Gupta, A. & Roughan, M.: Seasonal stratification and complex local dynamics control the sub-surface  
576 structure of marine heatwaves in Eastern Australian coastal waters. Commun Earth Environ, 4, 304, doi:10.1038/s43247-  
577 023-00966-4, 2023.

578 Simon, A., Plecha, S.M., Russo, A., Teles-Machado, A., Donat, M.G., Auger, P.-A., Trigo, R.M. : Hot and cold marine  
579 extreme events in the Mediterranean over the period 1982-2021. Front. Mar. Sci., 9:892201, doi:  
580 10.3389/fmars.2022.892201, 2022.

581 Ulses, C., Estournel, C. , Bonnin, J., Durrieu de Madron, X., Marsaleix, P. : Impact of storms and dense water cascading on  
582 shelf-slope exchanges in the Gulf of Lion (NW Mediterranean). Journal of Geophysical Research, 113, C02010, 2008.

583 Verdura, J., Linares, C., Ballesteros, E. et al.: Biodiversity loss in a Mediterranean ecosystem due to an extreme warming  
584 event unveils the role of an engineering gorgonian species. Sci. Rep., 9, 5911, doi:10.1038/s41598-019-41929-0, 2019.

585

586